Integral approximations in *ab initio*, electron propagator calculations

Roberto Flores-Moreno, and J. V. Ortiz

View Online   Export Citation

ARTICLES YOU MAY BE INTERESTED IN

Integral approximations in *ab initio*, electron propagator calculations

Roberto Flores-Moreno[1,2,a)] and J. V. Ortiz[1,b)]

[1]*Department of Chemistry and Biochemistry, Auburn University, Auburn, Alabama 36849-5312, USA*
[2]*Departamento de Química, Centro de Investigación y de Estudios Avanzados del Instituto Politécnico Nacional, Avenida Instituto Politécnico Nacional 2508, A.P. 14-740, México, D.F., C.P. 07000, Mexico*

Treatments of interelectronic repulsion that avoid four-center integrals have been incorporated in *ab initio*, electron-propagator calculations with diagonal self-energy matrices. Whereas the formal scaling of arithmetic operations in the propagator calculations is unaffected, the reduction of storage requirements is substantial. Moreover, the scaling of integral transformations to the molecular orbital base is lowered by one order. Four-index, electron-repulsion integrals are regenerated from three-index intermediates. Test calculations with widely applied self-energy approximations demonstrate the accuracy of this approach. Only small errors are introduced when this technique is used with quasiparticle virtual orbitals, provided that conventional techniques of integral evaluation are used in the construction of density-difference matrices. © *2009 American Institute of Physics*. [doi:10.1063/1.3238243]

I. INTRODUCTION

Electron propagator theory[1–5] (EPT) provides a foundation for the efficient and accurate evaluation of ionization energies and electron affinities of large molecules. Diagonal self-energy, or quasiparticle, approximations to the electron propagator are frequently used to determine correlation and relaxation corrections to Koopmans's theorem[6] results for the calculation of electron binding energies. Electrons assigned to canonical Hartree–Fock[7,8] (HF) orbitals are thereby subjected to a correlated, energy-dependent potential represented by the diagonal elements of the self-energy matrix. Several approximations of this kind have been characterized extensively in numerical tests and have been applied to many molecules and ions.[9–12]

Most implementations of many-body methods such as EPT are expressed in terms of formulae that involve electron repulsion integrals (ERIs) in the molecular orbital (MO) representation. For low-order perturbative approximations, one of the most computationally intensive tasks is the evaluation of these quantities. In conventional algorithms, ERIs in the MO base are stored on external disks. This strategy is advantageous provided that input/output operations are performed efficiently. At the cost of performing more arithmetic operations, direct or semidirect algorithms[13,14] may facilitate EPT calculations on larger species when disk storage of ERIs is infeasible. (The term direct refers to embedding the recalculation of ERIs in the formation of various intermediate matrices.) Transformation of ERIs from atomic-orbital (AO) to MO bases scales formally as N^5, where N is the dimension of the former base. Therefore, for many low-order, perturbative EPT methods, this transformation of four-index quantities constitutes the computational bottleneck, especially in conventional algorithms that avoid the recalculation of ERIs in the AO base.

Attempts to remove bottlenecks that arise from the rank of the ERI matrix may be founded on improved representations of electron densities or reductions in active orbital spaces. In the latter category, one finds a variety of improved virtual orbital techniques, such as a recent procedure that is based on density difference matrices that accompany low-order electron propagator methods.[15,16] In the former category, systematic elimination of redundant information in the base of electron densities generated by AOs is represented by the Cholesky decomposition approach.[17] Alternatives consider the expansion of AO-based densities in terms of auxiliary functions. Density fitting (DF) methodology played a prominent role in the development of programs that solve Kohn–Sham (KS) equations.[18] In correlated, *ab initio* calculations where numerous electron densities require representation, related strategies, dubbed resolution-of-the-identity (RI) methods, were successfully implemented.[19] Many recent publications considered the numerical calibration and relative advantages of Cholesky decomposition and RI techniques in the execution of well-known self-consistent field and perturbative methods.[20–28]

DF-RI methods offer a way to overcome arithmetic or storage obstacles to the execution of low-order, perturbative EPT calculations that arise, respectively, from integral transformation or the quantity of ERIs. To provide clear criteria for assessing the reliability of this approach, comparisons will be made with previous EPT calculations that employed HF reference states. Because the resulting algorithms do not require the evaluation of four-center ERIs in the AO base, they may be conveniently implemented in codes (see, for example, Ref. 29) that are designed chiefly for the solution of KS equations and that possess optimal routines for the evaluation of three-center integrals. This strategy also is ad-

a)Electronic mail: roberto.floresmoreno.qt@gmail.com.
b)Electronic mail: ortiz@auburn.edu.

vantageous for AO-based, molecular electron propagator calculations that employ KS reference determinants instead of their HF counterparts.[30]

This manuscript is organized as follows. In Sec. II, basic aspects of DF or RI techniques are discussed and their relevance to the execution of electron propagator calculations is established. The organization of the calculations is considered in Sec. III. In Sec. IV, the numerical performance of the method is analyzed for second-order and partial third-order quasiparticle approximations of EPT. Final remarks are given in Sec. V.

II. METHODS

A. ERIs in EPT formulae

In the diagonal, or quasiparticle, approximation to the electron propagator, the Dyson equation is reduced to

$$\omega_p = \epsilon_p + \Sigma_{pp}(\omega_p). \tag{1}$$

Here p labels a canonical, HF MO, ϵ_p is the corresponding energy, ω_p is the electron binding energy (ionization energy or electron affinity), and Σ_{pp} is a diagonal element of the energy-dependent, self-energy matrix. Up to first order in the fluctuation potential, the self-energy vanishes and the results of Koopmans's theorem are recovered for the ionization energy. For second order, the diagonal elements of the self-energy matrix are

$$\Sigma_{pp}^{[2]}(\omega_p) = \sum_{i,a<b} \frac{|\langle pi||ab\rangle|^2}{\omega_p + \epsilon_i - \epsilon_a - \epsilon_b} + \sum_{a,i<j} \frac{|\langle pa||ij\rangle|^2}{\omega_p + \epsilon_a - \epsilon_i - \epsilon_j}, \tag{2}$$

where i and j label only occupied MOs and a and b are used only for virtual orbitals. The brackets represent antisymmetrized ERIs in the MO representation. The threefold summations of Eq. (2) imply that arithmetic operations for the evaluation of second-order, self-energy matrix elements scale somewhat lower than N^3. Therefore, second-order calculations are highly efficient compared to self-consistent-field (SCF) iterations.

However, the evaluation of ERIs in the MO representation scales as N^5. MOs, φ, are built from linear combinations of atomic orbitals, μ, such that

$$\varphi_p(\mathbf{r}) = \sum_\mu C_{\mu p}\mu(\mathbf{r}), \tag{3}$$

and, therefore, evaluation of MO ERIs requires four transformation steps of the following type:

$$\langle p\nu||\sigma\tau\rangle = \sum_\mu C_{\mu p}\langle \mu\nu||\sigma\tau\rangle, \tag{4}$$

in which a Latin MO index supplants a Greek AO index. This step constitutes the bottleneck of many propagator calculations. If only one electron binding energy is needed, second-order calculations can be executed more efficiently by restricting the range of index p in Eq. (4) to a single value. The first step of the transformation generates intermediates with three running indices instead of four and there-

fore has N^4 arithmetic scaling. Each of the three subsequent steps has the same scaling factor.

For higher-order approximations such as partial third order[31] (P3) and the outer valence Green's function,[3,9] the pp self-energy matrix elements include terms with fivefold summations such as

$$\frac{1}{4}\sum_{abcij} \frac{\langle pa||ij\rangle\langle ij||bc\rangle\langle bc||pa\rangle}{(\omega_p + \epsilon_a - \epsilon_i - \epsilon_j)(\epsilon_i + \epsilon_j - \epsilon_b - \epsilon_c)}. \tag{5}$$

ERIs with no common p index are needed and a more general integral transformation must be executed. Even for the calculation of a single ionization energy, the transformation of the required integrals scales as N^5.

In conventional algorithms, MO ERIs are stored on disk and are recalled as needed in the evaluation of self-energy matrix elements. The resulting storage demands scale as N^4. In competing semidirect schemes, intermediates defined in terms of MO ERIs with four or three virtual orbital indices are generated through calculation of AO ERIs. For example, the intermediate X requires a subset of the MO ERIs with three virtual indices, where

$$X_{paij} = \sum_{bc} \frac{\langle ij||bc\rangle\langle bc||pa\rangle}{(\epsilon_i + \epsilon_j - \epsilon_b - \epsilon_c)}. \tag{6}$$

Such procedures may require repeated evaluations of AO ERIs.

B. Treatments of interelectronic repulsion

To reduce disk storage requirements and to avoid re-evaluation of AO ERIs, we consider alternatives based on DF or RI strategies. Antisymmetrized ERIs may be denoted as follows:

$$R_{st}^{pq} \equiv \langle pq||st\rangle = \langle pq|st\rangle - \langle pq|ts\rangle, \tag{7}$$

with

$$\langle pq|st\rangle = \int\int \frac{\varphi_p^*(\mathbf{r})\varphi_q^*(\mathbf{r}')\varphi_s(\mathbf{r})\varphi_t(\mathbf{r}')}{|\mathbf{r}-\mathbf{r}'|}d\mathbf{r}d\mathbf{r}'. \tag{8}$$

Here, p, q, s, and t are labels of molecular spin-orbitals and $\{\mathbf{R}^{pq}\}$ is a set of matrices that each contain a subset of ERIs with $\langle pq|$ in the *bra* space. The superscripts indicate only to which subset the matrix belongs. Spin is already integrated. Mulliken notation[32] also will be employed to establish relationships with DF-RI arguments, where

$$(ps|qt) \equiv \langle pq|st\rangle. \tag{9}$$

Mulliken notation has the advantage of separating the coordinates of the electrons. Such integrals are the ps matrix elements of the electrostatic potential generated by a single orbital product, qt. In DF-RI techniques,[18,19] orbital products are expressed as linear combinations of auxiliary functions, $\{g_k(\mathbf{r})\}$, where

$$\varphi_q(\mathbf{r})\varphi_t(\mathbf{r}) = \sum_k e_k^{qt}g_k(\mathbf{r}). \tag{10}$$

Once again, superscripts identify a pair of MOs that generates the potential that is being expanded in terms of auxiliary

functions. The latter functions will henceforth be assumed to be real. Left multiplication by a given function of the auxiliary set multiplied by the Coulomb operator,[19] $g_l(\mathbf{r}')/|\mathbf{r}-\mathbf{r}'|$, and integration over the full space of $\mathbf{r}$ and $\mathbf{r}'$ yields

$$(l|qt) = \sum_k e_k^{qt} G_{lk}, \tag{11}$$

with

$$(l|qt) \equiv \int \int \frac{g_l(\mathbf{r})\varphi_q^*(\mathbf{r}')\varphi_t(\mathbf{r}')}{|\mathbf{r}-\mathbf{r}'|} d\mathbf{r} d\mathbf{r}', \tag{12}$$

$$G_{lk} \equiv \int \int \frac{g_l(\mathbf{r})g_k(\mathbf{r}')}{|\mathbf{r}-\mathbf{r}'|} d\mathbf{r} d\mathbf{r}'. \tag{13}$$

Expansion coefficients may be computed according to

$$e_k^{qt} = \sum_l G_{kl}^{-1}(l|qt). \tag{14}$$

Therefore, four-index integrals are given by

$$(pr|qt) = \sum_{kl} (pr|k) G_{kl}^{-1}(l|qt). \tag{15}$$

Because the matrix $\mathbf{G}^{-1}$ is needed only at this level of the calculation, its absorption into three-index quantities can be exploited,[33] such that

$$T_{kt}^q \equiv \sum_l G_{kl}^{-1/2}(l|qt). \tag{16}$$

Here, only a single superscript labels the subset of three-center ERIs to which a given matrix $\mathbf{T}$ belongs. The dimensions of the matrix $\mathbf{T}^q$ are $M \times N$, where M is the number of auxiliary functions. M is, in general, a small multiple of N. Representative $M:N$ ratios for the GEN-A2* [34–37] auxiliary basis set are: 4:1 for cc-pVDZ, 3:1 for cc-pVTZ, and 2:1 for cc-pVQZ. This prefactor does not grow with the size of the system and, therefore, is not part of the formal scaling. Thus, four-index integrals may be obtained from simple matrix multiplications of three-index intermediates,

$$\mathbf{R}^{pq} = (\mathbf{T}^p)^\dagger \mathbf{T}^q - (\mathbf{T}^q)^\dagger \mathbf{T}^p. \tag{17}$$

Considerable economies of storage can be realized by saving $\mathbf{T}$ matrices on disk instead of the $\mathbf{R}$ matrices that occur in previous electron propagator algorithms. DF-RI techniques enable execution of conventional (as opposed to semidirect) algorithms in which all intermediates are stored on disk and AO ERIs need not be reevaluated. Moreover, the transformation from AO to MO bases can be executed for three-index matrices, $\mathbf{T}$, with a formal scaling of $M \times N^3$, thus gaining one order in the arithmetic scaling of this task according to

$$T_{kq}^p = \sum_\mu C_{\mu q} T_{k\mu}^p, \quad \forall p. \tag{18}$$

In DF-RI-EPT calculations beyond second order, the most intensive arithmetic task is calculation of self-energy matrix elements and not the transformation of integrals. Therefore, DF-RI-EPT calculations will not only reduce storage requirements, but can also compete in speed with previous algo-

rithms despite the need for extra integral evaluation and handling.

Note that the method described here does not use DF-RI for the SCF solution of the reference system. Such an approach would result in an approximate description of the self-energy's pole structure, for MO energies would be affected.[38] Preliminary calculations indicate that DF-RI approximations for the Coulomb contribution to the Fock matrix introduce deviations in orbital energies that are less than 0.01 eV. Nevertheless, simultaneous application of DF-RI approximations to SCF and EPT methods has not been attempted here, for procurement of HF wavefunctions does not constitute a bottleneck in EPT calculations.

III. COMPUTATIONAL DETAILS

All calculations were performed using the deMon2k program.[29] The two- and three-center integrals of Eqs. (12) and (13) are evaluated efficiently through employment of Hermite auxiliary functions.[39,40] Extra functionality was added to this program so that the modified version is able to evaluate four-center integrals and, therefore, to perform HF calculations. It can also execute EPT calculations of second order (EP2) and P3 in the quasiparticle approximation. An interface routine builds four-index ERIs in the MO base by using deMon2k routines for evaluation of two- and three-center ERIs. Auxiliary function sets are generated automatically for each choice of basis set.[34–37] Two basis sets commonly employed in EPT calculations were used: cc-pVTZ[41] for small molecules and 6-311G(d,p) [42,43] for porphyrin.

IV. RESULTS AND DISCUSSION

A. Size dependence of errors

The present DR-RI techniques are intended for the study of large molecules where ordinary EPT calculations are infeasible. Here, the behavior of errors introduced by these techniques as a function of molecular size is examined. A plot of such errors versus the number of carbons in alkane chains is shown in Fig. 1. For these calculations, the cc-pVDZ and auxiliary GEN-A2* basis sets were used. After an initial maximum for ethane, the error declines through heptane and increases only slightly for octane. There is no evidence that errors grow in proportion to chain length. Unlike the results of Ref. 44, where DF-RI was applied in a different
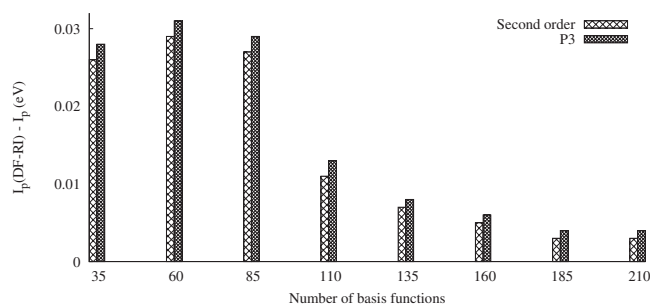

FIG. 1. Variation of error in ionization energies with respect to *n*-alkane chain length.

TABLE I. Accuracy of RI-EP2 for small molecules.

Molecule	Orbital	RI-EP2		EP2[a]	Expt.[a]
		GEN-A2	GEN-A2*		
B_2H_6	$1b_{3g}$	12.066	12.208	12.21	11.9
CH_4	$1t_2$	14.026	14.060	14.07	14.40
C_2H_4	$1b_{3u}$	10.455	10.328	10.33	10.51
	$1b_{3g}$	12.656	12.747	12.75	12.85
	$3a_g$	14.477	14.482	14.48	14.66
	$1b_{2u}$	15.847	15.882	15.89	15.87
	$2b_{1u}$	19.270	19.334	19.34	19.23
HCN	1π	13.778	13.678	13.68	13.61
HNC	1π	13.856	13.746	13.74	12.55
NH_3	$3a_1$	10.244	10.167	10.17	10.8
N_2	$1\pi_u$	17.149	17.049	17.05	16.98
	$3\sigma_g$	15.034	15.022	15.02	15.60
	$2\sigma_u$	18.192	18.197	18.20	18.78
CO	5σ	14.045	14.056	14.06	14.01
	1π	16.485	16.371	16.37	16.91
H_2CO	$2b_2$	9.936	9.938	9.94	10.9
H_2O	$1b_1$	11.615	11.500	11.50	12.78
	$3a_1$	13.945	13.862	13.86	14.74
	$1b_2$	18.137	18.085	18.08	18.51
HF	1π	14.841	14.708	14.70	16.19
	3σ	19.043	18.945	18.94	20.00
F_2	$1\pi_g$	14.301	14.205	14.20	15.83
	$3\sigma_g$	20.643	20.470	20.46	21.1
	$1\pi_u$	17.451	17.358	17.35	18.8
MAD vs Expt.		0.574	0.613	0.615	0.000
MAD vs EP2		0.081	0.042	0.000	

[a]See Ref. 12.

context, the approach presented here is stable with respect to the size of the system, provided that auxiliary basis sets of good quality are used.

B. Accuracy for small molecules

DF-RI methods also may be judged by their accuracy for valence ionization energies of small molecules. Tables I and II compare conventional results[12] with their DF-RI counterparts in the second order (EP2) and P3 quasiparticle approximations. The same cc-pVTZ basis sets and molecular structures were employed in both sets of calculations. Mean absolute deviations (MADs) of the DF-RI results with respect to the conventional data are below 0.1 eV for GEN-A2 and below 0.05 eV for GEN-A2* auxiliary basis sets. MADs with respect to experimental values are no worse for the use of the DF-RI methods.

C. Improved virtual orbitals

In a recent publication, we described a novel method for the reduction of the virtual orbital space in quasiparticle electron propagator calculations.[15,16] Substantial computational efficiencies achieved through the construction of quasiparticle virtual orbitals (QVOs) generally produced only small

deviations from electron binding energies obtained with the full set of unoccupied orbitals. Here we consider DF-RI calculations performed with QVOs. It is necessary to evaluate elements of the density-difference matrix described in Ref. 15,

$$\Delta\rho^p_{ab} = \delta_{ap}\delta_{bp} - \sum_{j<k} \frac{\langle pa||jk\rangle\langle jk||pb\rangle}{(E_p + \epsilon_a - \epsilon_j - \epsilon_k)(E_p + \epsilon_b - \epsilon_j - \epsilon_k)}$$
$$+ \sum_{jc} \frac{\langle pj||ac\rangle\langle bc||pj\rangle}{(E_p + \epsilon_j - \epsilon_a - \epsilon_c)(E_p + \epsilon_j - \epsilon_b - \epsilon_c)}, \quad (19)$$

with conventional techniques based on four-center ERIs. Preliminary tests performed with DF-RI methods for the construction of the density difference matrix indicate that extra errors appear in corresponding P3 calculations with an active virtual space that is 50% as large as the original. Therefore, if the QVOs procedure is employed, DF-RI methods should be activated only after the reduction of the virtual orbital space is realized. Fortunately, exact, four-center ERIs required for the determination of the density difference matrix can be computed with N^4 arithmetic scaling. Storage requirements for intermediate matrices scale as N^3. These scaling factors are the same as those of the DF-RI procedure. Results from Ref. 15 with 100% (i.e., no QVO reduction) or 50% retentions of virtual orbitals are compared with analogous DF-RI calculations in Table III. For the 100% case, the MAD of P3

TABLE II. Accuracy of RI-P3 for small molecules.

Molecule	Orbital	RI-P3		P3[a]	Expt.[a]
		GEN-A2	GEN-A2*		
B_2H_6	$1b_{3g}$	11.984	12.137	12.14	11.9
CH_4	$1t_2$	14.177	14.219	14.22	14.40
C_2H_4	$1b_{3u}$	10.676	10.554	10.55	10.51
	$1b_{3g}$	12.877	12.968	12.98	12.85
	$3a_g$	14.878	14.883	14.89	14.66
	$1b_{2u}$	16.067	16.102	16.11	15.87
	$2b_{1u}$	19.362	19.433	19.44	19.23
HCN	1π	14.061	13.957	13.96	13.61
HNC	1π	14.220	14.112	14.11	12.55
NH_3	$3a_1$	10.802	10.729	10.73	10.8
N_2	$1\pi_u$	17.286	17.186	17.18	16.98
	$3\sigma_g$	15.938	15.929	15.93	15.60
	$2\sigma_u$	19.286	19.302	19.30	18.78
CO	5σ	14.255	14.270	14.27	14.01
	1π	17.155	17.044	17.04	16.91
H_2CO	$2b_2$	10.901	10.899	10.90	10.9
H_2O	$1b_1$	12.613	12.494	12.49	12.78
	$3a_1$	14.859	14.773	14.77	14.74
	$1b_2$	18.794	18.740	18.74	18.51
HF	1π	16.085	15.944	15.94	16.19
	3σ	19.944	19.841	19.84	20.00
F_2	$1\pi_g$	15.734	15.625	15.62	15.83
	$3\sigma_g$	21.223	21.047	21.04	21.1
	$1\pi_u$	18.999	18.892	18.89	18.8
MAD vs Expt.		0.248	0.249	0.250	0.000
MAD vs P3		0.084	0.037	0.000	

[a]See Ref. 12.

results produced by the DF-RI method is 0.003 eV. When the dimension of the virtual orbital space is reduced by 50%, this deviation is 0.008 eV. The mean effect of employing both approximations (50% QVOs and DF-RI) is 0.086 eV for P3 calculations. Therefore, DF-RI methods can be combined with QVOs for the treatment of even larger molecules.

D. Porphyrin

Recent electron propagator studies of porphyrins and their derivatives[45,46] provide a suitable standard of comparison for DF-RI techniques. P3/6-311G** calculations generated a consistent and accurate assignment of the lowest ion-

TABLE III. Effects of RI methods on P3/cc-pVTZ ionization energies (eV) obtained with QVOs (50%) and full virtual orbital (100%) spaces.

Molecule	Orbital	50%		100%	
		P3[a]	RI-P3	P3[a]	RI-P3
Benzene	e_{1g}	9.362	9.363	9.402	9.403
	e_{2g}	12.166	12.167	12.302	12.298
	a_{2u}	12.321	12.348	12.384	12.385
	e_{1u}	14.362	14.359	14.466	14.462
	b_{2u}	15.000	15.004	15.066	15.067
	b_{1u}	15.636	15.628	15.757	15.750
	a_{1g}	17.197	17.187	17.314	17.310
Borazine	e''	10.290	10.295	10.318	10.320
	e'	11.682	11.676	11.825	11.820
	a_2''	12.847	12.850	12.906	12.907
	a_1'	13.926	13.908	14.037	14.030
	e'	15.079	15.065	15.152	15.150
	a_2'	14.872	14.869	14.929	14.930
	e'	17.848	17.835	17.905	17.904
RI-MAD			0.008		0.003

[a]Reference 15.

TABLE IV. Ionization energies (eV) of free porphyrin in RI calculations with GEN-A2 auxiliary functions.

Orbital	KT	P3[a]	RI-P3	Expt.[a]
a_u	6.14	7.02	7.078	7.1
b_{1u}	6.66	6.96	7.031	6.9
b_{3g}	9.13	8.30	8.368	8.4
b_{1u}	9.30	8.48	8.550	8.4

[a]See Ref. 45.

ization energies of porphyrin. The results of Table IV indicate the DF-RI technique, executed with the GEN-A2 auxiliary basis set, introduces deviations from ordinary P3 calculations that are less than 0.07 eV. The DF-RI results are all slightly larger those of Ref. 45 by 0.05–0.07 eV and provide a consistent account of the cationic final states.

V. CONCLUSIONS

DF or RI techniques have been proposed as a means to performing *ab initio* electron propagator calculations on large systems. Test calculations on small molecules, alkanes, benzene, borazine, and porphyrin show that employment of standard auxiliary functions may enable calculations of triple-ζ plus polarization quality to be executed without unacceptable loss of accuracy. Significant reductions in external disk storage and decreased arithmetic operations for the bottleneck of ordinary calculations, the four-index integral transformation, have been achieved. These techniques may be combined with methods for reducing the rank of the virtual orbital space, provided that conventional ERI techniques are employed in the evaluation of density-difference matrices. Applications to larger molecules on modestly constructed computational platforms lie in prospect.

ACKNOWLEDGMENTS

[1] J. Linderberg and Y. Öhrn, *Propagators in Quantum Chemistry*, 2nd ed. (Wiley-Interscience, Hoboken, New Jersey, 2004).

[2] P. Jørgensen and J. Simons, *Second-Quantization Based Methods in Quantum Chemistry* (Academic, New York, 1981).

[3] W. von Niessen, J. Schirmer, and L. S. Cederbaum, Comput. Phys. Rep. **1**, 57 (1984).

[4] M. F. Herman, K. F. Freed, and D. L. Yeager, Adv. Chem. Phys. **48**, 1 (1981).

[5] J. V. Ortiz, Adv. Quantum Chem. **35**, 33 (1999).

[6] T. Koopmans, Physica **1**, 104 (1933).

[7] D. R. Hartree, Proc. Cambridge Philos. Soc. **24**, 328 (1928).

[8] V. A. Fock, Z. Phys. **15**, 126 (1930).

[9] J. V. Ortiz, in *Computational Chemistry: Reviews of Current Trends*, edited by J. Leszczynski (World Scientific, Singapore, 1997).

[10] J. V. Ortiz, V. G. Zakrzewski, and O. Dolgounitcheva, in *Conceptual Perspectives in Quantum Chemistry*, edited by J.-L. Calais and E. S. Kryachko (Kluwer, Dordrecht, 1997).

[11] A. M. Ferreira, G. Seabra, O. Dolgounitcheva, V. G. Zakrzewski, and J. V. Ortiz, in *Quantum–Mechanical Prediction of Thermochemical Data*, edited by J. Cioslowski (Kluwer, Dordrecht, 2001).

[12] R. Flores-Moreno, V. G. Zakrzewski, and J. V. Ortiz, J. Chem. Phys. **127**, 134106 (2007).

[13] V. G. Zakrzewski and J. V. Ortiz, Int. J. Quantum Chem., Quantum Chem. Symp. **28**, 23 (1994).

[14] V. G. Zakrzewski and J. V. Ortiz, Int. J. Quantum Chem. **53**, 583 (1995).

[15] R. Flores-Moreno and J. V. Ortiz, J. Chem. Phys. **128**, 164105 (2008).

[16] O. Dolgounitcheva, R. Flores-Moreno, V. G. Zakrzewski, and J. V. Ortiz, Int. J. Quantum Chem. **108**, 2862 (2008).

[17] N. H. F. Beebe and J. Linderberg, Int. J. Quantum Chem. **12**, 683 (1977).

[18] J. L. Whitten, J. Chem. Phys. **58**, 4496 (1973); J. W. Mintmire, Int. J. Quantum Chem. **13**, 163 (1979); B. I. Dunlap, J. W. D. Connolly, and J. R. Sabin, J. Chem. Phys. **71**, 4993 (1979); J. W. Mintmire and B. I. Dunlap, Phys. Rev. A **25**, 88 (1982).

[19] M. Feyereisen, G. Fitzgerald, and A. Komornicki, Chem. Phys. Lett. **208**, 359 (1993); O. Vahtras, J. Almlöf, and M. W. Feyereisen, *ibid.* **213**, 514 (1993).

[20] F. Aquilante, T. B. Pedersen, and R. Lindh, J. Chem. Phys. **126**, 194106 (2007).

[21] F. Aquilante, R. Lindh, and T. B. Pedersen, J. Chem. Phys. **127**, 114107 (2007).

[22] F. Aquilante and T. B. Pedersen, Chem. Phys. Lett. **449**, 354 (2007).

[23] I. Røeggen and T. Johansen, J. Chem. Phys. **128**, 194107 (2008).

[24] F. Aquilante, T. B. Pedersen, R. Lindh, B. O. Roos, A. Sánchez de Merás, and H. Koch, J. Chem. Phys. **129**, 024113 (2008).

[25] L. Boman, H. Koch, and A. Sánchez de Merás, J. Chem. Phys. **129**, 134107 (2008).

[26] F. Aquilante, L. Gagliardi, T. B. Pedesen, and R. Lindh, J. Chem. Phys. **130**, 154107 (2009).

[27] J. Zienau, L. Clin, B. Doser, and C. Ochsenfeld, J. Chem. Phys. **130**, 204112 (2009).

[28] F. Weigend, M. Kattannek, and R. Ahlrichs, J. Chem. Phys. **130**, 164106 (2009).

[29] A. M. Köster, P. Calaminici, M. E. Casida, V. D. Domínguez, R. Flores-Moreno, G. Geudtner, A. Goursot, T. Heine, A. Ipatov, F. Janetzko, J. M. del Campo, S. Patchkovskii, J. U. Reveles, A. M. Vela, B. Zúñiga, and D. R. Salahub, deMon2k, the International deMon Developers Community, México, 2008.

[30] Y. Shigeta, A. M. Ferreira, V. G. Zakrzewski, and J. V. Ortiz, Int. J. Quantum Chem. **85**, 411 (2001).

[31] J. V. Ortiz, J. Chem. Phys. **104**, 7599 (1996).

[32] A. Szabo and N. S. Ortlund, *Modern Quantum Chemistry* (Dover, Mineola, New York, 1996).

[33] A. P. Rendell and T. J. Lee, J. Chem. Phys. **101**, 400 (1994).

[34] J. Andzelm, E. Radzio, and D. R. Salahub, J. Comput. Chem. **6**, 520 (1985).

[35] J. Andzelm, N. Russo, and D. R. Salahub, J. Chem. Phys. **87**, 6562 (1987).

[36] P. Calaminici, R. Flores-Moreno, and A. M. Köster, Comput. Lett. **1**, 164 (2005).

[37] P. Calaminici, F. Janetzko, A. M. Köster, R. Mejía-Olvera, and B. Zúñiga-Gutiérrez, J. Chem. Phys. **126**, 044108 (2007).

[38] S. Hamel, M. E. Casida, and D. R. Salahub, J. Chem. Phys. **114**, 7342 (2001).

[39] A. M. Köster, J. Chem. Phys. **104**, 4114 (1996).

[40] A. M. Köster, J. Chem. Phys. **118**, 9943 (2003).

[41] T. H. Dunning, J. Chem. Phys. **90**, 1007 (1989).

[42] R. Krishnan, J. S. Binkley, R. Seeger, and J. A. Pople, J. Chem. Phys. **72**, 650 (1980).

[43] M. J. Frisch, J. A. Pople, and J. S. Binkley, J. Chem. Phys. **80**, 3265 (1984).

[44] C.-K. Skylaris, L. Gagliardi, N. C. Handy, A. G. Ioannou, S. Spencer, and A. Willetts, J. Mol. Struct.: THEOCHEM **229**, 501 (2000).

[45] O. Dolgounitcheva, V. G. Zakrzewski, and J. V. Ortiz, J. Am. Chem. Soc. **127**, 8240 (2005).

[46] O. Dolgounitcheva, V. G. Zakrzewski, and J. V. Ortiz, J. Phys. Chem. A **109**, 11596 (2005).